

Quantum Corrected Boltzmann Transport Model for Tunneling Effects

Bo Wu and Ting-wei Tang

Department of Electrical and Computer Engineering, University of Massachusetts
 Marcus Hall, UMass, Amherst, MA 01003, USA
 Phone: +413-545-4762 Email: bwu@ecs.umass.edu Fax: +413-545-4611

Abstract—A quantum correction method based on the effective total potential used for the Monte Carlo simulation is presented. The Bohm-based and Wigner-based quantum correction models are unified under a single effective conduction-band edge (ECBE) method via a density-dependent quantum correction coefficient. The ECBE equation in thermal equilibrium as well as nonequilibrium is derived. This new equation is then applied to the MC simulation of quantum tunneling of a step potential barrier.

I. INTRODUCTION

The Boltzmann transport equation (BTE) using the ensemble Monte Carlo (MC) method has been successfully applied to semiconductor device simulations for many decades. However, quantum mechanical (QM) effects such as carrier confinement and barrier tunneling cannot be properly described by the semi-classical BTE. A few techniques have been developed in order to bring quantization and tunneling effects into classical simulations. The effective potential method [1] incorporates quantum effects associated with the finite-size of the electron into classical simulations. Another quantum MC method is based on the Wigner function formalism in which the dynamics of particles are treated classically with a nonlocal quantum force [2]. The density-gradient (DG) method [3] includes the quantum effects arising from the density gradient and is equivalent to Madelung-Bohm-Takabayasi's [4,5,6] interpretation of the Schrödinger equation. All of these methods have advantages and disadvantages. In this work, the Wigner-based and the Bohm-based quantum correction models are unified and a new method based on the effective conduction-band edge (ECBE) is presented.

II. THE BOHM-BASED AND WIGNER-BASED QUANTUM CORRECTION MODELS

For stationary states, the substitution of the wave function into the single-particle Schrödinger equation yields [5]

$$E = V(\vec{r}) - \frac{\hbar^2}{4m} \left[\frac{\nabla^2 P}{P} - \frac{1}{2} \frac{(\nabla P)^2}{P^2} \right] \quad (1)$$

where $P(\vec{r}) = R^2(\vec{r})$ and $\psi = R \cdot \exp(iS/\hbar)$ is the wave function in complex form. For a pure state, the probability density $P(\vec{r})$ is proportional to the carrier density $n(\vec{r})$. Under this assumption, (1) becomes

$$\begin{aligned} E &\approx V(\vec{r}) - \frac{\hbar^2}{4m} \left[\nabla^2 \ln n(\vec{r}) + \frac{1}{2} (\nabla \ln n(\vec{r}))^2 \right] \\ &= V(\vec{r}) - \frac{\hbar^2}{2m} \frac{\nabla^2 \sqrt{n}}{\sqrt{n}} = V(\vec{r}) + V_B^Q(\vec{r}). \end{aligned} \quad (2)$$

Since the Bohm quantum potential V_B^Q depends on the density gradient, the quantum correction based on (2) is also known as the DG method.

The Wigner-based quantum correction model can be derived from the Wigner transport equation (WTE) [7]. By retaining the lowest order term in $O(\hbar^2)$, the WTE becomes the QM corrected BTE,

$$\begin{aligned} \frac{\partial f}{\partial t} + \vec{v} \cdot \nabla_r f - \frac{1}{\hbar} \nabla_r V \cdot \nabla_k f \\ + \frac{1}{\hbar} \nabla_r V_w^Q \cdot \nabla_k f = \left(\frac{\partial f}{\partial t} \right)_c \end{aligned} \quad (3)$$

where the Wigner quantum potential V_w^Q is often approximated by [8-11]

$$V_w^Q(\vec{r}) \approx -\frac{\hbar^2}{8m} \nabla^2 \ln n(\vec{r}) \text{ or } -\frac{\hbar^2}{12m} \nabla^2 \ln n(\vec{r}). \quad (4)$$

However, the correct expression for V_w^Q should be [7, 12, 13]

$$V_w^Q(\vec{r}) \approx \frac{\hbar^2}{12mk_B T} \left[\nabla^2 V(\vec{r}) - \frac{1}{2} \frac{1}{k_B T} (\nabla V(\vec{r}))^2 \right]. \quad (5)$$

Note that there is a difference between (4) and (5). Missing a term proportional to $(\nabla V(\vec{r}))^2$ in (5) significantly affects the Wigner-based quantum correction model.

If we were to assume $n(\vec{r}) \propto \exp\left(-\frac{V(\vec{r})}{k_B T}\right)$, (5) becomes

$$\begin{aligned} V_w^Q(\vec{r}) &\approx -\frac{\hbar^2}{12m} \left[\nabla^2 \ln n(\vec{r}) + \frac{1}{2} (\nabla \ln n(\vec{r}))^2 \right] \\ &= -\frac{\hbar^2}{6m} \frac{\nabla^2 \sqrt{n}}{\sqrt{n}}. \end{aligned} \quad (6)$$

Since V_B^O and V_W^O are similar at lowest order in $O(\hbar^2)$ except for a numerical factor of 2 or 3, we do not need to treat them separately. In unifying these two quantum potentials, we define the effective total potential (ETP) $V^*(\bar{r}) = V(r) + V^O(\bar{r})$ [5-6]. Basically, the eigenenergy E in (2) plays the role of the effective total potential energy $V^*(\bar{r})$, or in other words, the role of the ECBE, $E_c^*(\bar{r})$. In this hydrodynamic picture, the kinetic energy part of the Hamiltonian is transferred to the potential energy part $V(\bar{r})$ and considered as a quantum potential or “self-potential” [6]. Thus, (2) and (6) can be combined and rewritten as

$$V^*(\bar{r}) = V(r) - \frac{\hbar^2}{4mr} \left[\nabla^2 \ln n(\bar{r}) + \frac{1}{2} (\nabla \ln n(\bar{r}))^2 \right], \quad (7)$$

where with $r=1$, V^* represents the effective total Bohm potential, V_B^* , and with $r=3$, it represents the effective total Wigner potential, V_W^* .

In recent years, (4) has recently been used extensively in the QM corrected Monte Carlo (MC) simulation of semiconductor devices, notably by Tsuchiya and his co-workers [2, 11, 14-17]. In this approach, particles are not accelerated by the conventional electrostatic force $F(\bar{r}) = -\nabla V(\bar{r})$ but rather by the QM corrected force $F^*(\bar{r}) = -\nabla V^*(\bar{r})$ which includes the quantum effect through the density gradient. However, aside from the use of an incorrect Wigner potential, the MC calculated carrier density in this approach suffers from statistical fluctuations and it is difficult to obtain an accurate $F^*(\bar{r})$, which involves a third spatial derivative of $n(\bar{r})$.

III. THE EFFECTIVE CONDUCTION-BAND EDGE EQUATION

To circumvent the difficulty associated with the density fluctuations, we propose the following: For the equilibrium Boltzmann distribution, after the quantum correction, $\ln n(\bar{r})$ is proportional to $-V^*(\bar{r})/k_B T$ and not to $-V(\bar{r})/k_B T$. With this proper connection between $n(\bar{r})$ and $V^*(\bar{r})$, (7) can be transformed into the following second-order differential equation for $V^*(\bar{r})$:

$$V^*(\bar{r}) = V(r) + \frac{\hbar^2}{4mrk_B T} \left[\nabla^2 V^*(\bar{r}) - \frac{1}{2} \frac{1}{k_B T} (\nabla V^*(\bar{r}))^2 \right], \quad (8)$$

which we will call the ETP field equation or the ECBE equation valid under the equilibrium condition. We believe such an equation has never been presented.

In fact, the Bohm and Wigner-based models can be unified if r in (8) is replaced by a density dependent $r(n)$ given by

$$r(n) = \sqrt{\pi} N_C [F_{-1/2}(\eta)]^2 / [2n(dF_{-1/2}(\eta)/d\eta)] \quad (9)$$

which is related to $12h(n) = 1/[2r(n)]$ listed in Appendix B of Perrot [18]. Figure 1 shows how r varies with n .

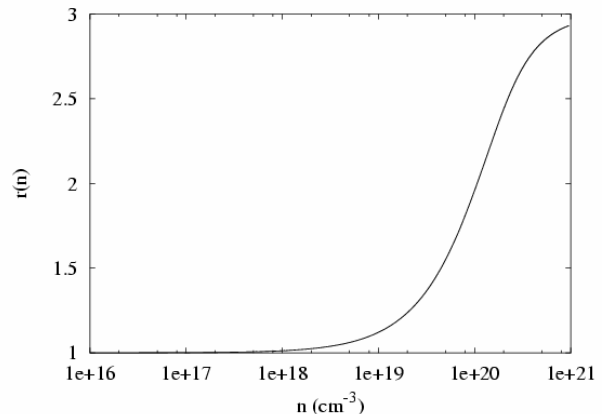


Figure 1: $r(n)$ vs electron density.

When the carrier transport is involved, i.e., under the non-equilibrium condition, $n(\bar{r})$ is no longer proportional to $\exp[-V^*(\bar{r})/k_B T]$ and (8) has to be modified. In addition to satisfying (7), both n and V^* must be self-consistent with a set of quantum hydrodynamic (QHD) equations. The lowest-order moment of the QHD equations in which F^* appears is the momentum conservation equation,

$$\frac{\partial(n\bar{P})}{\partial t} + \nabla \cdot (n\hat{U}) - n\bar{F}^* = n\bar{C}_p, \quad (10)$$

where $\bar{P} = \langle \hbar k \rangle$ is the crystal momentum, $\hat{U} = \langle \hat{v} \hbar k \rangle$ is the energy stress tensor, $\bar{F}^* = -\nabla(V + V^O) = -\nabla V^*$ is the QM corrected force, and $\bar{C}_p = \langle \hbar k (\partial f / \partial t)_{coll} \rangle$ is the average rate of change of momentum due to collisions [19]. Equation (10) is similar to Takabayasi's QHD model for the Schrödinger field [6], except that the QM stress $\sigma_{kl} = (\hbar^2/4m) \frac{\partial^2 (\ln R^2)}{\partial x_l \partial x_k}$ is transferred to the potential V to become an effective total potential V^* . For a steady-state problem and assuming $\hat{U} = U\hat{I}$ for simplicity, (10) reduces to

$$\nabla(\ln n) = -U^{-1} \nabla V^* - \nabla \ln U + U^{-1} \bar{C}_p. \quad (11)$$

The elimination of $\nabla(\ln n)$ from (7) and (11) yields

$$\begin{aligned} & \nabla^2 V^* + \nabla^2 U - \nabla \cdot \bar{C}_p \\ & - \frac{1}{2} \frac{1}{U} (\nabla V^*)^2 - \frac{3}{2} U (\nabla \ln U)^2 - \frac{1}{2} \frac{1}{U} C_p^2 \\ & - 2 \nabla(\ln U) \cdot \nabla V^* + \frac{1}{U} \nabla V^* \cdot \bar{C}_p + 2 \nabla(\ln U) \cdot \bar{C}_p \end{aligned}$$

$$= \frac{4}{\lambda_{th}^2 r(n)} \frac{U}{k_B T} (V^* - V), \quad (12)$$

where $\lambda_{th}^2 = \frac{\hbar^2}{mk_B T}$. This is our 3-D ECBE equation valid under the biased conditions. If we assume $U \approx k_B T = const.$, then (12) in 1-D becomes

$$\frac{d^2 V^*}{dx^2} - \frac{1}{2} \frac{1}{k_B T} \left(\frac{dV^*}{dx} \right)^2 + \frac{1}{k_B T} \frac{dV^*}{dx} \cdot C_p - \frac{dC_p}{dx} - \frac{1}{2} \frac{1}{k_B T} C_p^2 = \frac{4}{\lambda_{th}^2 r} (V^* - V). \quad (13)$$

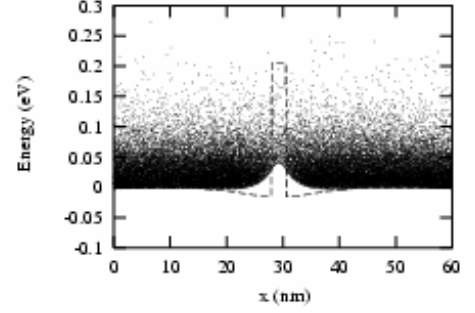
This equation is the same as Ancona's D-G drift-diffusion model if C_p is expressed in terms of a mobility [20]. Equation (12) for V^* (or E_C^*) must be solved at each field adjustment time the same way Poisson's equation is solved for V . Similar to inputting $n(\vec{r})$ from the MC simulation when solving Poisson's equation, data for U and C_p must be input from the MC simulation when solving the field equation for V^* . However, unlike the DG method in which the density gradient is directly evaluated from the MC simulation, the solution for V^* is always smooth and stable because (12) is integrated twice.

IV. SIMULATION PROCEDURES

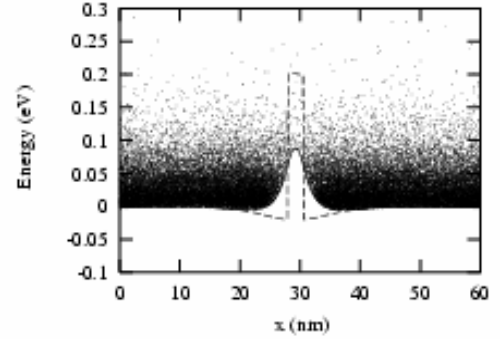
As a demonstration for the application of the ECBE equation, we consider 1-D tunneling of a GaAs/AlGaAs/GaAs barrier with a barrier height of 0.22 eV and a barrier width of 2.5 nm. For the unbiased case, we use (8) for the calculation of $V^*(x)$. We choose $r=1$ and $r=3$ to compare the Bohm-based and Wigner-based quantum corrections. The electrostatic potential barrier $V(x)$ is updated self-consistently by solving Poisson's equation at each 0.2fs. At the same time, (8) is solved for $V^*(x)$. A newly calculated QM force $F_x^* = -dV^*(x)/dx$ is then used to advance particles. For the biased case, we solve (12) in 1-D. Two approximations are used here for the purpose of comparison. In lieu of (12), one approximation uses (8) while the other uses (8) but with $k_B T$ replaced by U which must be input from the MC simulation.

V. SIMULATION RESULTS AND DISCUSSION

Fig. 2 shows electron distributions in space and energy of the GaAs/AlGaAs/GaAs single barrier at zero bias using the flat band voltage. As can be seen, both quantum correction models show quantum repulsion by the potential barrier but the barrier height resulted from the Bohm model ($r=1$) is substantially lower than that from the Wigner model ($r=3$). Fig. 3 compares self-consistent solutions of electron distribution obtained by the Bohm-based MC solution and the calculated $n \propto \exp(-V^*(\vec{r})/k_B T)$ using (8) at zero-bias. The two curves follow each other very closely, which indicates that the relationship $\ln n(\vec{r}) \propto -V^*(\vec{r})/k_B T$ is indeed correct.



(a)



(b)

Figure 2: A snapshot of the electron distribution in space and energy at zero-biased condition. (a) Bohm model. (b) Wigner model using (8)

Figure 4 shows the ETP obtained under the unbiased condition using (8). The model with $r=1$ produces a slightly narrower barrier width and a substantially lower barrier height than that obtained from the model with $r=3$ as seen in Fig. 2. Also included in Fig. 4 is the ETP obtained by using a self-consistent quantum correction coefficient $r(n)$ and the result obtained is very close to that obtained by the model using $r=1$ in (8). Figure 5 shows the ETP at the bias voltage of 0.05V.

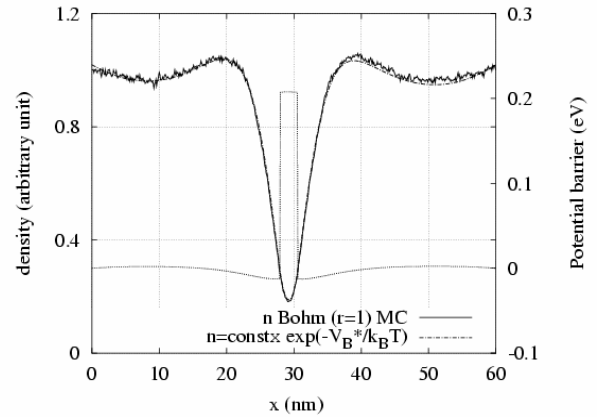


Figure 3: Electron density vs position.

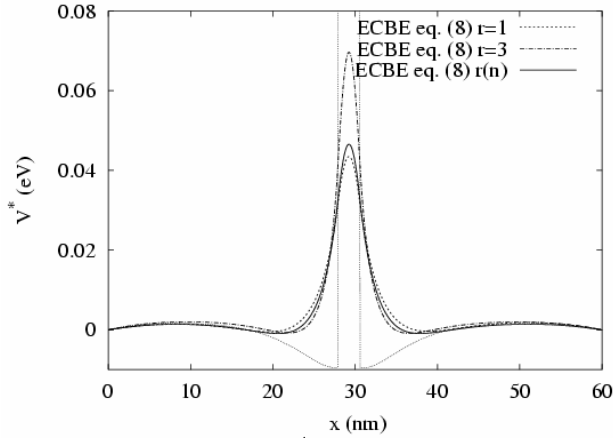


Figure 4: Comparison of V^* obtained by different ECBE models at zero bias.

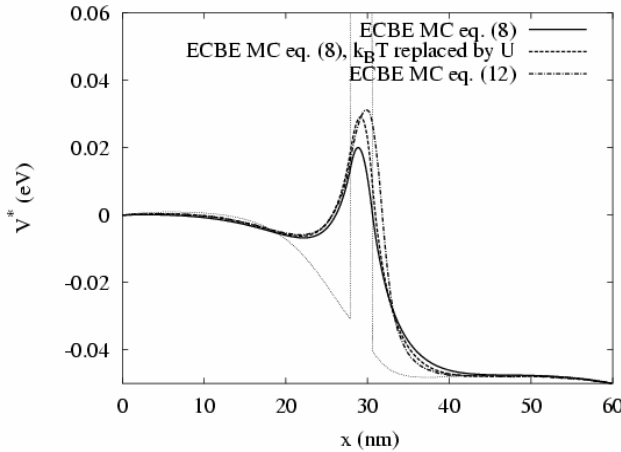


Figure 5: V^* obtained by different ECBE models at a bias of 0.05V.

The barrier height obtained by the equilibrium ECBE model using (8) (the first approximation) is lower than that obtained by the nonequilibrium ECBE model using (12). Equation (8) with $k_B T$ replaced by U (the second approximation) produces an ECBE barrier height similar to that produced by (12). The barrier height obtained by using (8), (12), and (8) with $k_B T$ replaced by U are 0.0200, 0.0291 and 0.0311 eV, respectively. The corresponding current densities are 7.73×10^{-3} , 5.48×10^{-3} and $5.03 \times 10^{-3} A/\mu m^2$, respectively. It is interesting to note that the ratios of current density $7.73/5.48 = 1.41$ and $5.48/5.03 = 1.09$ corresponds exactly to the ratios $\exp[(0.0291 - 0.0200)/0.0259] = 1.42$ and $\exp[(0.0311)/0.0291] = 1.08$, as should be expected. Note also that the peak of the effective barrier V_{\max}^* shifts to the right from the center of the barrier to the edge of the conduction-band discontinuity when (12) is used instead of (8). This is in

agreement with the earlier work of Frensley [21] using the discrete Wigner distribution function model.

VI. CONCLUSIONS

We have proposed a new field equation from which the ETP, V^* (or the ECBE, E_C^*) can be solved. This potential is then used to calculate the quantum force employed in the classical MC solution of the BTE. The main advantage of calculating V^* is to avoid the density fluctuations arising from the MC simulation. Both Bohm and Wigner quantum potentials are unified under a single ECBE model. The ECBE model with $r=r(n)$ produces reasonable results to the barrier tunneling under the biased conditions. Application of this ECBE method to the full and quasi-2-D simulation of practical devices such as FinFETs and DGMOSFETs will be published soon.

ACKNOWLEDGMENT

This work is supported in part by NSF Grant ECS-0120128.

REFERENCES

- [1] D.K. Ferry, Superlett. Microstruct. **28**, 419 (2000).
- [2] H. Tsuchiya and U. Ravaioli, J. Appl. Phys. **89**, 4023 (2001).
- [3] M.G. Ancona and H.F. Tiersten, Phys. Rev **B35**, 7959 (1987).
- [4] E. Madelung, Z. Phys., **40**, 322 (1926).
- [5] D. Bohm, Phys. Rev. **85**, 166 (1952).
- [6] T. Takayabasi, Prog. Theo. Phys. **8**, 143 (1952).
- [7] E. Wigner, Phys. Rev. **40**, 749 (1932)
- [8] G. J. Iafrate, H. L. Grubin and D. K. Ferry, J. Phys. Colloq. C7, **42**, 307 (1981).
- [9] M. G. Ancona and G. J. Iafrate, Phys. Rev. **B39**, 9536 (1989).
- [10] H. L. Grubin, J. P. Kreskovsky, T. R. Govindan and D. K. Ferry, Semicond. Sci. Technol. **9**, 855 (1994).
- [11] H. Tsuchiya and T. Miyoshi, IEICE Trans. Electron. **E82-C**, 880 (1999).
- [12] H. L. Grubin and J. P. Kreskovsky, Solid-State Electron. **32**, 1071 (1989).
- [13] H. L. Grubin, T. R. Govindan and J. P. Kreskovsky, Solid-State Electron. **36**, 1697 (1993).
- [14] H. Tsuchiya and U. Ravaioli, J. Appl. Phys. **89**, 4023 (2001).
- [15] B. Winstead, H. Truchiya and U. Ravaioli, J. Compt. Electron. **1**, 201 (2002).
- [16] H. Truchiya and U. Ravaioli, J. compt. Electron. **1**, 295 (2002).
- [17] M. Ogawa, H. Tsuchiya and T. Miyoshi, IEICE Trans. Electron. **E86-C**, 1 (2003).
- [18] F. Perrot, Phys. Rev. **A20**, 586 (1979).
- [19] M. K. Jeong and T.-w. Tang, IEEE Trans. Electron Device **44**, 2242 (1997).
- [20] M. G. Ancona, COMPEL, **6**, 11 (1987).
- [21] W. R. Frensley, Rev. Mod. Phys. **62**, 745.